



THE UNIVERSITY *of* EDINBURGH

Edinburgh Research Explorer

Analysis of EEG networks and their correlation with cognitive impairment in preschool children with epilepsy

Citation for published version:

Kinney-lang, E, Yoong, M, Hunter, M, Kamath Tallur, K, Shetty, J, McLellan, A, Chin, R & Escudero, J 2019, 'Analysis of EEG networks and their correlation with cognitive impairment in preschool children with epilepsy', *Epilepsy & behavior : E&B*, vol. 90, pp. 45-56. <https://doi.org/10.1016/j.yebeh.2018.11.011>

Digital Object Identifier (DOI):

[10.1016/j.yebeh.2018.11.011](https://doi.org/10.1016/j.yebeh.2018.11.011)

Link:

[Link to publication record in Edinburgh Research Explorer](#)

Document Version:

Peer reviewed version

Published In:

Epilepsy & behavior : E&B

General rights

Copyright for the publications made accessible via the Edinburgh Research Explorer is retained by the author(s) and / or other copyright owners and it is a condition of accessing these publications that users recognise and abide by the legal requirements associated with these rights.

Take down policy

The University of Edinburgh has made every reasonable effort to ensure that Edinburgh Research Explorer content complies with UK legislation. If you believe that the public display of this file breaches copyright please contact openaccess@ed.ac.uk providing details, and we will remove access to the work immediately and investigate your claim.



Analysis of EEG networks and their correlation with cognitive impairment in preschool children with epilepsy

Eli Kinney-Lang^{a,b,*}, Michael Yoong^b, Matthew Hunter^b, Krishnaraya Kamath Tallur^c, Jay Shetty^c, Ailsa McLellan^c, Richard FM Chin^{†b,c}, Javier Escudero^{†a,b}

^a*School of Engineering, Institute for Digital Communications, The University of Edinburgh, Edinburgh EH9 3FB, United Kingdom*

^b*The Muir Maxwell Epilepsy Centre, The University of Edinburgh, Edinburgh EH8 9XD, United Kingdom*

^c*Royal Hospital for Sick Children, Edinburgh EH9 1LF, United Kingdom*

Abstract

Objective: Cognitive impairment (CI) is common in children with epilepsy and can have devastating effects on their quality of life. Early identification of CI is a priority to improve outcomes, but the current gold standard of detection with psychometric assessment is resource intensive and not always available. This paper proposes exploiting network analysis techniques to characterize routine clinical electroencephalography (EEG) to help identify CI in children with early-onset epilepsy (CWEOE) (0-5 y.o.).

Methods: Functional networks from routinely acquired EEGs of 51 newly diagnosed CWEOE were analyzed. Combinations of connectivity metrics with sub-network analysis identified significant correlations between network properties and cognition scores via rank correlation analysis (Kendall's τ). Predictive properties were investigated using a cross-validated classification model with normal cognition, mild/moderate CI and severe CI classes.

Results: Network analysis revealed phase-dependent connectivity having higher sensitivity to CI, and significant functional network changes across EEG frequencies. Nearly 70.5% of CWEOE were aptly classified as normal cognition, mild/moderate CI or severe CI using network features. These features predicted CI classes 55% better than chance and halved misclassification penalties.

Conclusions: CI in CWEOE can be detected with sensitivity at 85% (in identifying mild/moderate or severe CI) and specificity of 84%, by network analysis.

Significance: This study outlines a data-driven methodology for identifying candidate biomarkers of CI in CWEOE from network features. Following additional replication, the proposed method and its use of routinely acquired EEG forms an attractive proposition for supporting clinical assessment of CI.

*Corresponding author

† Authors contributed equally to the work.

Email address: e.kinney-lang@ed.ac.uk (Eli Kinney-Lang)

Keywords: Network analysis, signal processing, EEG graph networks, paediatric epilepsy, developmental impairment

Highlights

- EEG network analysis correlates with CI in preschool children with epilepsy
- Classification reveals network features' predictive potential for CI identification
- Sensitivity to CI improves with dense networks and phase-based connectivity measures

1. Introduction

Epilepsy is a complex disease that can have devastating effects on quality of life [1]. Cognitive impairment (CI), which frequently and severely affects quality of life of children and their families, coexists in more than half of children with epilepsy [2, 3, 4, 5]. Timely identification of CI, particularly in children with early-onset epilepsy (CWEEOE; epilepsy onset < 5 years of age) is critical because early-life interventions are likely to be more effective, it is the period in which childhood epilepsy is most common, and the most severe forms occur during this time [6, 7, 8]. An estimated 40% of CWEEOE have CI [5]. The urgent need for emphasis on early recognition, new interventions and improved public health strategies for primary and secondary prevention for CI in epilepsy is highlighted in calls to action by august bodies including the International League Against Epilepsy, The Institute of Medicine, and the World Health Organization [9, 10]. Therefore, there is a need to understand the causes of CI and find reliable, affordable and non-invasive markers beyond current standard approaches.

Identification of CI is especially difficult in CWEEOE because the gold standard of diagnosis by psychological assessments may not be readily available [11], it is resource intensive, and can be clinically challenging (e.g. introducing potential bias from repeated testing) [11]. Thus, reliable, affordable and rapid CI screening techniques in clinical care are sought after. Such techniques would help focus further medical investigations and resources onto a smaller subgroup, producing efficiency gains and cost savings. Graph network analysis of standard routine clinical EEG recordings is one such potential technique.

Analysis of functional EEG networks offers a data-driven methodology for understanding diverse brain conditions through the lens of network (connectivity) properties [12, 13]. Functional networks examined as graphs are well-established, and provide advantages in understanding changes in connectivity across the brain, e.g. through exploiting properties like small-world topology, connected hubs and modularity [13, 14, 15, 16, 17]. Insights into epilepsy, including the severity of cognitive disturbances, outcomes of epilepsy surgery, and

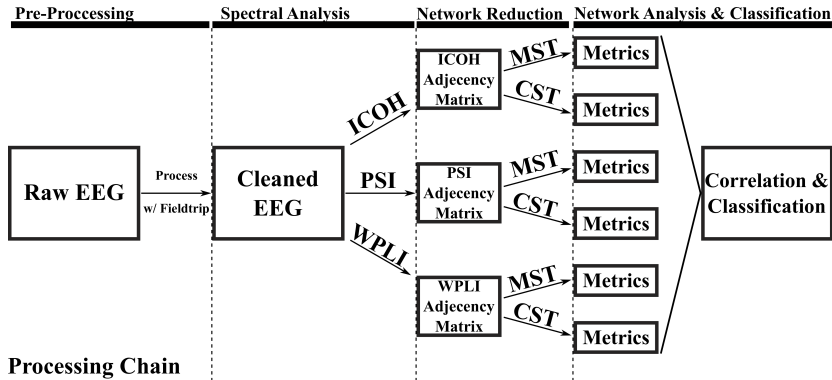


Figure 1: Flowchart of data processing chain for an individual child. ICOH = Imaginary part of coherency, PSI = Phase-slope index, WPLI = Weighted phase-lag index, MST = Minimum Spanning Tree, CST = Cluster-Span Threshold

32 disease duration have been found to correlate with the extent of changes in these
 33 functional networks [18]. Recent work has also found network abnormalities can
 34 appear in both ictal and interictal states [18]. This supports that network can
 35 be distinguished in resting-state EEG [18]. Therefore, functional graph analysis
 36 is well positioned as a potential tool to reveal insights into CI in CWEOE.

37 The aim of this study was to identify a reliable EEG network marker which
 38 could help effectively screen for CI in CWEOE. Our hypothesis was two-fold.
 39 First, informative network abnormalities relating to CI could be revealed in
 40 CWEOE using graph network analysis on routine clinical EEGs. Second, identified
 41 abnormalities could be integrated into a simple machine learning paradigm
 42 to demonstrate predictive capabilities of the identified networks with respect to
 43 CI. We aimed to utilize a data-driven, quantitative approach to identify potential
 44 network markers. Then, we could integrate their information into a simple
 45 classification pipeline, which could be readily implemented to support clinical
 46 decisions regarding CI. By investigating only routine EEG recordings, we
 47 hoped to demonstrate that minimal potential cost and effort would be required
 48 to adopt the proposed techniques into a clinical setting.

49 2. Methods

50 The data processing pipeline for each child is summarized in Figure 1.

51 2.1. Dataset

52 The details on study recruitment and assessments are reported elsewhere
 53 [19]. In summary, newly diagnosed CWEOE of mixed epilepsy types and aetiologies
 54 were recruited as part of a prospective population-based study of neurodevelopment
 55 in CWEOE [20]. Parents gave approval for use of the standard, resting-state,
 56 awake 10-20 EEG their child had as part of their routine clinical care. If a
 57 child had multiple EEGs, only the first EEG was used to avoid biasing

58 results toward children with multiple recordings. Additionally, it allowed similar
59 selection of resting-state recordings across all children, e.g. awake resting-state.
60 As such, no EEG recordings of sleep were analysed in this work. All analy-
61 ses were blinded to any treatment or seizure frequency information. Partici-
62 pants underwent cognitive assessment with age-appropriate standardized tools,
63 e.g. Bayley Scales of Infant and Toddler Development- Third Edition (Bayley-
64 III) and Wechsler Preschool and Primary Scale of Intelligence-Third Edition
65 (WPPSI-III). Children who scored within ± 1 standard deviation (SD) of the
66 normative mean were defined as normal, -1 to -2 SD as having mild/moderate
67 CI, and < -2 SD as having severe CI. The cognition scores from Bayley-III and
68 WPPSI-III tests were converted into a normalized standard score measure. Clin-
69 ical details were collected by members of the research team using a standardized
70 proforma by direct interview of care-givers, medical records and, where possi-
71 ble, patients themselves when they attended for clinical and/or research study
72 assessment.

73 Table 1 provides the demographic and clinical features for the CWEOE
74 which were included in this study. Given the broad anti-epileptic drug (AED)
75 therapies and aetiologies present in Table 1, potential interactions from AED
76 load or specific aetiology were examined with respect to the designated CI classes
77 (e.g. normal, mild/moderate, severe CI). Using a non-parametric version of
78 the two-way ANOVA (Friedman’s test [21]) on data from Table 1, revealed no
79 significant interactions between any AED load or specific aetiology with respect
80 to any CI classes. This in turn suggests that the results identified via network
81 analysis are likely driven mainly by cognitive phenomena, as opposed to epileptic
82 syndrome or AED load effects.

83 A retrospective analysis was done on 32-channel, unipolar montage with
84 average reference captured routine EEGs. EEGs were recorded at 20 scalp
85 electrodes (FP1, FP2, FPz, F3, F4, F7, F8, Fz, C3, C4, Cz, P3, P4, Pz, T3,
86 T4, T5, T6, O1, O2), eight auxiliary electrodes (AUX1-8), two grounding (A1,
87 A2) and two ocular electrodes (PG1, PG2).

88 *2.2. Pre-processing*

89 EEG recordings were pre-processed in MATLAB using the Fieldtrip tool-
90 box [22]. The EEG had a sampling rate of approximately 511 Hz. Recordings
91 were re-referenced to a common average reference (CAR), and bandpass fil-
92 tered between 0.5-45 Hz in Fieldtrip. The resting-state data was split into non-
93 overlapping, two second long sub-trials; long enough to pick up any resting-state
94 network activity, while still fitting at least one full period of the lowest included
95 frequency.

96 Prior to data processing, seizure activity in the EEGs were confirmed by
97 clinicians. Whole trials which contained seizure activity were excluded from
98 the analysis, rather than excluding only sections of trials with evident seizure
99 activity. This helped guarantee that all network trials were derived from a
100 minimum of two continuous seconds of seizure-free EEG. The small time window
101 helped to balance removing large amounts of useful EEG data, while retaining
102 enough data to characterize the frequencies present.

	Normal ($n = 31$)	Mild/Moderate CI ($n = 7$)	Severe CI ($n = 13$)
Age in months (SD)	36.18 (19.87) [†]	26.76 (17.06)	20.37 (18.56) [†]
Male:Female Ratio	20:11	6:1	6:7
Ethnicity			
Asian	2 (6%)	–	1 (8%)
Black	–	1 (14%)	–
White (U.K./European)	29 (94%)	6 (86%)	12 (92%)
Antiepileptic Drugs			
None	3 (10%)	1 (14%)	–
Monotherapy	26 (84%)	6 (86%)	9 (69%)
Polytherapy	2 (6%)	–	4 (31%)
Focal Seizures	12 (39%)	3 (43%)	4 (31%)
Generalized Seizures	18 (58%)	2 (28%)	9 (69%)
Generalized and Focal	1 (3%)	2 (28.5%)	–
Epilepsy aetiology			
Cryptogenic	3 (10%)	1 (14%)	5 (38%)
Idiopathic	24 (77%)	4 (57%)	1 (8%)
Symptomatic	3 (10%)	2 (29%)	7 (54%)
Unknown	1 (3%)	–	–
Cognitive z -score (SD)	-0.05 (0.66)	-1.41 (0.20)	-2.9 (0.27)

Table 1: Demographic and clinical feature information of patients, grouped by CI classes of normal, mild/moderate CI, and severe CI. Significant differences between groups with respect to age are indicated by a [†] (Kruskal-Wallis with post-hoc Mann-Whitney U; $H = 6.4697$, $p < 0.05$, with mean ranks of 30, 23.7143, and 17.6923 for Normal, Mild/Moderate CI and Severe CI respectively.)

103 Standard EEG artefacts were rejected using a 2-step approach with manual
104 and automatic rejection. Manual artefact rejection first removed clear outliers
105 in both trial and channel data based upon high variance values ($var > 10^6$).
106 Muscle, jump and ocular artefacts were then automatically identified using strict
107 rejection criteria relative to the Fieldtrip default suggested values [22] (Fieldtrip
108 release range R2015-R2016b, z -value rejection level $r = 0.4$). All trials contain-
109 ing EEG artefacts were excluded from analysis. Subjects were averaged across
110 all trials at each frequency band to help reduce potential bias and variance
111 resulting from the selection of a shorter analysis window.

112 A narrow band (2-Hz wide) approach was used in analysis of clean EEG
113 data, similar to work done by Miskovic et al. [23]. Segmenting the frequency
114 range into these narrow bands (e.g. 1-3 Hz, 3-5 Hz,...) provided a data-driven
115 approach to interrogate networks across subjects. The a priori nature of the in-
116 vestigation avoided attempts at equivocating the (likely heterogeneous) impact
117 of epilepsy, development, medication etc. on each child’s spectral EEG compo-
118 sition. While such narrow bands may eschew some physiological interpretations
119 by not adhering to classical frequency bands, the narrow bands promoted iden-
120 tification of mainly robust, common network abnormalities across the heteroge-
121 neous CWEOE population. If significant network abnormalities were identified
122 in these narrow frequency bands (after correction for multiple comparisons, age
123 and spurious correlations) then the identified results were likely representative
124 of a strong effect.

125 *2.3. Network Coupling Analysis*

126 The processed data was analyzed using functional EEG graph analysis, based
127 on ‘functional links’ connecting any pair of EEG channels i and j , derived from
128 the cross-spectrum of the data. Appendix A provides the detailed, formal def-
129 initions for the cross-spectrum and the network analysis methods described
130 below. A summary of these definitions are included here for clarity. In brief,
131 this study selected several measures of dependencies in EEG recordings, cre-
132 ated graph networks based on these measures and characterized the created
133 networks to identify candidate biomarkers for classification and identification of
134 CI in CWEOE.

135 This study investigates three connectivity analysis methods building from
136 the cross-spectrum viz: (1) the imaginary part of coherency (ICOH) [24], (2)
137 phase-slope index (PSI) [25], and (3) weighted phase-lag index [26, 27].

138 ICOH is a standard measure in functional network analysis [24]. ICOH is
139 well documented, and has been shown to provide direct measures of true brain
140 interactions from EEG while eliminating self-interaction and volume conduction
141 effects [24]. A weakness of ICOH, however, is its dependence on phase-delays,
142 resulting in identifying functional connections only at specific phase differences
143 between signals, while completely failing for others [26, 27, 28].

144 The PSI [25] was selected as a complementary alternative to ICOH for anal-
145 ysis. In practice, the PSI examines causal relations (temporal order) between
146 two sources for signals of interest, e.g. s_i and s_j [25]. PSI exploits the phase
147 differences between the sources to identify the ‘driving’ versus ‘receiving’ re-
148 lationship between the sources [25]. Their average phase-slope differences are
149 used to identify functional links [25]. Importantly, unlike ICOH, the PSI is
150 equally sensitive to all phase differences from cross-spectral data [25]. However,
151 the PSI equally weights contributions from all phase differences, meaning even
152 small phasic perturbations are equal to the (defining) large perturbations.

153 Therefore the weighted phase-lag index (WPLI) was included as a third compar-
154 ative measurement for analysis [26, 27]. The standard phase-lag index (PLI)
155 [26] is a robust measure derived from the asymmetry of instantaneous phase
156 differences between two signals, resulting in a measure which is less sensitive to
157 volume conduction effects and independent of signal amplitudes [26]. The PLI
158 ranges between 0 and 1, where PLI of zero indicates no coupling (or coupling
159 with a specific phase difference; see [26] for details), and a PLI of 1 indicates
160 perfect phase locking [26]. The PLI’s sensitivity to noise, however, is hindered
161 as small perturbations can turn phase lags into leads and vice versa [27].

162 A weighted version of the PLI was introduced (weighted PLI; WPLI) [27]
163 to counter this effect. The WPLI adds proportional weighting based on the
164 imaginary component of the cross-spectrum [27]. The proportional weighting
165 alleviates the noise sensitivity in PLI. The WPLI, like the PSI, helps capture
166 potential phase-sensitive connections present in EEG networks from another
167 perspective.

168 *2.4. Adjacency Matrices and Sub-Networks*

169 The estimated functional connectivity between channel pairs i and j com-
170 prising the weighted functional network of a subject can be represented by an
171 adjacency matrix. The functional connections found for the ICOH, PSI, and
172 WPLI measures were therefore represented via adjacency matrices in the analy-
173 sis below. A set of adjacency matrices for a representative normal and impaired
174 cognition child in the range of 5-9 Hz are included in Appendix B, Figures B.5
175 and B.6, respectively.

176 Constructing and comparing graphs of functional EEG networks built using
177 the adjacency matrix can lead to certain biases in the network analysis [29,
178 30, 31]. To avoid this issue, two methods for defining unbiased sub-networks
179 to represent the functional EEG for comparison and analysis were used: the
180 Minimum Spanning Tree (MST) [29] and the Cluster-Span Threshold (CST)
181 [32].

182 The MST is an acyclic, sub-network graph which connects all nodes (elec-
183 trodes) of a graph while minimizing link weights (connectivity strength) based
184 on applying Kruskal’s algorithm on the weighted network [29, 33]. In brief,
185 the algorithm first orders the link weights in a descending manner, i.e. from
186 strongest to weakest connectivity [29]. The MST is then constructed by start-
187 ing with the largest link weight and adding the next largest link weight until
188 all nodes, N , are connected in an acyclic sub-network with a fixed density of
189 $M = N - 1$ [29]. After construction of the sub-network, all weights are assigned
190 a value of one [29]. In this manner, the MST is able to efficiently capture a
191 majority of essential properties underlying a complex network in an unbiased
192 sub-network [29].

193 Exploiting the properties of the MST is a relatively recent technique, pre-
194 sented in contemporary publications exploring brain networks [29]. However,
195 the MST naturally leads to sparse networks in the data due to its acyclic nature
196 and, in some occasions, more dense networks may be preferable. Thus, real
197 brain network information is potentially lost in MST based EEG graph analysis
198 [34].

199 By contrast, the CST creates a similar sub-network, but balances the pro-
200 portion of cyclic ‘clustering’ (connected) and acyclic ‘spanning’ (unconnected)
201 structures within a graph (for details see [32]). This balance thus retains nat-
202 urally occurring ‘loops’ which can reflect dense networks without potential in-
203 formation loss [34] while maintaining the advantages of using an unbiased sub-
204 network for analysis. Figure 2 illustrates a topographical example of EEG chan-
205 nels connected via MST and CST networks for a randomly selected child. Differ-
206 ences in sparsity between the acyclic MST and the cyclic CST sub-networks can
207 readily be seen in Figure 2. Both the MST and CST are binary sub-networks
208 and consequently have advantages over weighted networks like the adjacency
209 matrix, e.g. spurious connections and link density effects [29, 32, 34].

210 For each combination of sub-networks and connectivity definitions above
211 (e.g. MST-ICOH, CST-ICOH, MST-PSI, etc.) four network metrics were in-
212 vestigated for correlation to the cognition standard score measures. To help

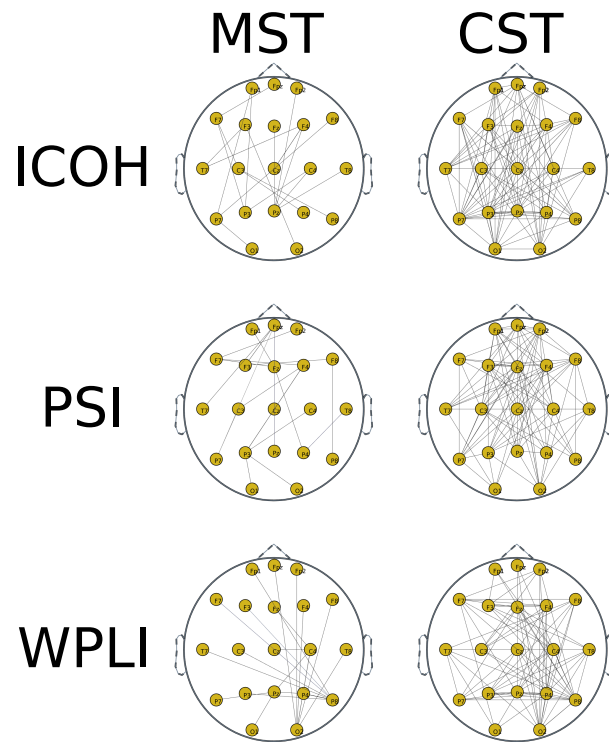


Figure 2: Illustrative examples of the MST and CST sub-network graphs of ICOH, PSI and WPLI for a randomly selected child. EEG channels are displayed as nodes, with functional connections displayed for each combination of sub-network and connectivity measure.

213 reduce potential selection bias, network metrics for analysis were agreed upon a
214 priori. Metrics were chosen to account for distinct network properties (e.g. the
215 shape of the network, the critical connection points in the network etc.) with
216 (relatively) little inter-correlation. Due to the natural exclusion/inclusion of cy-
217 cles, the network metrics differ for the MST and CST, respectively. However, all
218 metrics across sub-networks were selected to be comparable regarding network
219 properties. Pictorial examples of the selected network metrics, alongside short
220 definitions, are given in Figure 3.

221 2.5. Statistical Analysis

222 Statistical analysis was done using Matlab 2015a. Correlation between in-
223 dividual network metrics and the cognition standard score was measured using
224 Kendall’s tau (τ) [35]. Kendall’s τ calculates the difference between concordant
225 and discordant pairs [35, 36], and is a strong choice for describing correlation
226 in ordinal or ranking properties. In this work, the normalized cognition stan-
227 dard scores’ relative rankings serve as the ordered data explored using the τ
228 correlation. The design of Kendall’s τ is also relatively robust to false posi-
229 tive correlations from data outliers [35, 36], providing additional mitigation
230 to spurious correlations in the results. Furthermore, as Kendall’s τ is a non-
231 parametric hypothesis test it did not rely on any underlying assumptions about
232 the distribution of the data. Therefore the correlation analysis was robust to
233 any potential ceiling, floor or skewed distribution effects present in the reported
234 cognition standard score measures.

235 Correlation trends are reported both as uncorrected $p < 0.05$ values, and
236 with multiple comparison (Bonferroni) corrections, similar in style to previous
237 literature [37]. For each frequency bin (2-Hz wide) and network, we compared
238 and corrected for the 4 separate graph measures using the Bonferroni technique
239 (i.e. $p = 0.05/4 = 0.0125$ was set as the threshold for significance). Dependency
240 was assumed across the small 2-Hz frequency bins, similar in principle to [37],
241 and as such we do not include the frequency bins in the Bonferroni correction.
242 Correlations which are found to be potentially significant under this assumption
243 are indicated by the \dagger symbol for Bonferroni corrections.

244 2.6. Classification

245 A multi-class classification scheme was devised using the Weka toolbox [38,
246 39]. Class labels of *normal*, *mild/moderate CI*, and *severe CI* were applied.

247 Primary feature selection included all correlations identified by the statisti-
248 cal analysis, thereby promoting interpretation of the retained network features.
249 Then, a second feature selection phase using nested 5-fold cross-validation se-
250 lected prominent features via bi-directional subspace evaluation [40]. Within
251 this nested cross-validation, features identified as important in $> 70\%$ of the
252 folds were selected for use in classification.

253 Due to the natural skew of the data (towards normalcy), and the context
254 of the classification problem (e.g. misclassifying different classes has various
255 implications), a cost-sensitive classifier was developed [41]. In order to properly

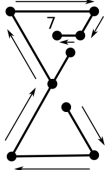
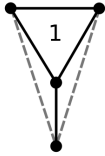
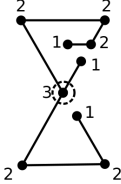
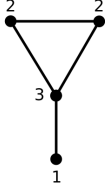
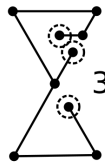
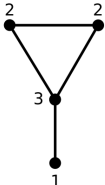
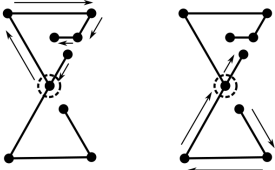
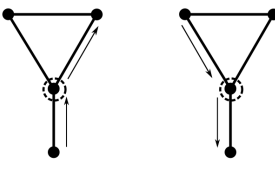
MST	CST
<p>Diameter: The longest 'shortest path' from any two nodes</p>  <p>= 7</p>	<p>Clustering Coefficient: Formed 'clustering' triangles out of all possible triangle clusters (max)</p>  <p>= 1/4</p>
<p>Max Degree: The node with the largest number of connecting edges</p>  <p>= 3</p>	<p>Average Degree: The average degree of all graph nodes</p>  <p>= 2</p>
<p>Leaf Fraction: The fraction of the total nodes with degree = 1</p>  <p>$3/9 = 1/3$</p>	<p>Variance Degree: The variance of all degree values in a graph</p>  <p>= 1/2</p>
<p>Betweenness Centrality: Measures 'centrality' of nodes with respect to various shortest paths</p> 	<p>Betweenness Centrality: Measures 'centrality' of nodes with respect to various shortest paths</p> 

Figure 3: Illustration of all graph analysis metrics for the Minimum Spanning Tree (MST) and Cluster-Span Threshold (CST) networks using simple example graphs. Nodes (dots) represent EEG channel electrodes. Edges (lines) represent functional interactions between EEG channels identified by a connectivity measure, e.g. ICOH/PSI/WPLI.

Multi-class Classification Cost Matrix

		CI-Predicted Class		
		Normal	Mild/Mod.	Severe
CI-True Class	Normal	0	2.5	2.5
	Mild/Mod.	5	0	1
	Severe	5	1	0

Table 2: Weighted cost matrix for misclassification of cognitive impairment (CI) for normal (± 1 SD), mild/moderate (-1 to -2 SD) and severe (< -2 SD) classes. Rows represent true class labels, with columns as the predicted classification labels.

256 develop such a classifier, an appropriate cost matrix needed to be identified.
 257 Using guidelines outlined in the literature [41], the cost matrix in Table 2 was
 258 developed, with predicted classes represented on the rows and real classes given
 259 on the columns.

260 The defined matrix satisfies several key concerns in multi-class cost-matrix
 261 development [41]. The weights on misclassification were carefully selected to
 262 reflect probable clinical concerns in classification with guidance from paediatric
 263 neurologists (RC, JS). The cost for incorrectly classifying an impaired child as
 264 normal was twice as heavy compared to misclassifying a normal child into either
 265 impaired group. This was still significantly more punishing than if impairment
 266 was correctly identified but misclassification occurred in determining between
 267 mild/moderate or severe impairment. These weighted values prioritized accu-
 268 rately including as many ‘true positive’ CWEOE with CI first, i.e. increasing
 269 sensitivity, followed by a secondary prioritization on being able to discern the
 270 level of CI. These boundaries provide a more clinically relevant classification
 271 context in the analysis.

272 Using the selected features and developed cost-sensitive matrix, a nested
 273 5-fold cross-validation trained a simple K -Nearest Neighbour (KNN) classifier,
 274 with $N = 3$ neighbours and Euclidean distance to minimize the above costs. By
 275 demonstrating the proof-of-concept results with KNN, we aimed to demonstrate
 276 significant network responses found from the proposed analysis pipeline could
 277 be exploited using a simple to implement (and interpret) classification scheme.
 278 Other potential (and more complex) classifiers are given some consideration
 279 in the *Discussion* section below. A repeated ‘bagging’ (Bootstrap Aggregation
 280 [42]) approach was used to reduce variance in the classifier at a rate of 100
 281 iterations/fold. Results were evaluated upon their overall classification accuracy
 282 and total penalty costs (e.g. sum of all mistakes based on the cost matrix).

283 Random classification and naive classification (e.g. only choosing a single
 284 class for all subjects) were included for comparison. In this study, random clas-
 285 sification refers to classification of any ‘true’ class label to a randomly selected
 286 ‘predicted’ class label. Based on the distribution of subjects into the classes, a
 287 ‘chance’ level for each class is used to assign the ‘predicted’ label at random.
 288 Naive classification (e.g. single-class classification), assumes that all subjects
 289 belong to only one class. Classification accuracy and misclassification penalties
 290 are then calculated based on the presumed (single) class assignment. This study

291 looked at naive classification for each class label, and have reported comparisons
292 to each possible naive classification.

293 **3. Results**

294 Of 64 children enrolled into the parent study, 13 were excluded from the
295 current study due to corrupted EEG data and inconsistent or incompatible EEG
296 acquisition parameters. There were data available for analysis on 51 children
297 (32:19 male-to-female ratio, mean age and SD of 30.85 ± 20.08 months). On
298 average approximately 455 ± 325 two second trials were used for each child in
299 the analysis, totalling 15.16 ± 11.87 minutes of resting-state EEG data for each
300 child. Thirty-one children had normal cognition, 7 had mild/moderate CI, and
301 13 had severe CI.

302 *3.1. Correlation Analysis*

303 Each combination of functional link analysis (ICOH/PSI/WPLI) and sub-
304 network selection (MST/CST) techniques uncovered likely correlations between
305 at least one network metric (outlined in Figure 3) and the cognition standard
306 score measures. A summary of the significant correlations between the MST
307 metrics and the standard scores are shown in Table 3. All MST correlations
308 were in the medium to high frequency range, 9 – 31 Hz, with no significant
309 results in lower frequencies. Activity above approximately 9 Hz is outside of the
310 expected range for the delta, theta and alpha bands in young children [43, 44].
311 Sets of contiguous frequency bands with significant correlations were found in
312 the ICOH and PSI connectivity measures, and are reported together as a single
313 frequency range. Overlapping correlations retained at significant levels after
314 partial correlation correcting for age are also reported for the MST using a
315 modified Kendall’s τ .

316 Similarly, significant correlations between the CST metrics and the cogni-
317 tion standard scores are shown in Table 4. Several significant CST metrics exist
318 in the lower frequency range (< 9 Hz), indicating a potential sensitivity of the
319 CST to lower frequencies. No sets of continuous frequency bands were discov-
320 ered, but several sets were trending towards this phenomenon within ICOH.
321 Multiple overlapping correlations remaining after partial correlation correction
322 for age from the modified τ in the CST at lower frequencies indicate additional
323 sensitivity.

324 Both the MST and CST demonstrate high sensitivity in the phase-dependent
325 measures (PSI, WPLI) compared to the standard ICOH.

326 *3.2. KNN Classification*

327 Based upon CST’s sensitivity, a preliminary classification scheme assessed
328 the potential predictive qualities of the CST network metrics in identifying CI
329 classes. The relative quality of the classifications are examined using classifica-
330 tion accuracy and total ‘cost’ (i.e. penalty for misidentification) [41].

MST analysis of cognition standard score measures			
Network Type	Network Measurement	Frequency Range(s) (Hz)	Correlation ($\bar{\tau} \pm SD$)
ICOH	Diameter	–	–
ICOH	Maximum Degree	–	–
ICOH	Leaf Fraction	–	–
ICOH	Betweenness Centrality	13-17 Hz	-0.231 ± 0.001
PSI	Diameter	9-19 Hz	$0.239 \pm 0.032^{\dagger*}$
PSI	Maximum Degree	11-13 Hz	$-0.232 \pm 0.000^*$
PSI	Maximum Degree	15-17 Hz	$-0.258 \pm 0.000^*$
PSI	Maximum Degree	21-23 Hz	-0.219 ± 0.000
PSI	Leaf Fraction	11-13 Hz	-0.201 ± 0.000
PSI	Leaf Fraction	15-19 Hz	-0.246 ± 0.003
PSI	Betweenness Centrality	9-13 Hz	$-0.218 \pm 0.012^*$
PSI	Betweenness Centrality	17-19 Hz	$-0.259 \pm 0.000^{\dagger*}$
WPLI	Diameter	–	–
WPLI	Maximum Degree	29-31 Hz	$-0.310 \pm 0.000^{\dagger*}$
WPLI	Leaf Fraction	–	–
WPLI	Betweenness Centrality	23-25 Hz	0.223 ± 0.000

Table 3: Summary of Kendall’s τ correlation trends between various graph metrics and the cognition standard scores using the Minimum Spanning Tree (MST). For all values $|\tau|$ was between 0.201 and 0.310; mean = 0.239 ± 0.0278 and uncorrected $p < 0.05$. Significant values across contiguous narrow-band frequencies have been grouped together for ease of interpretation.

[†] Significant with Bonferroni correction at the level of frequencies.

* Significant after partial correlation correction to age of subjects, via modified τ with uncorrected $p < 0.05$.

331 The subset of CST metrics for classification, identified from significant cor-
332 relations and chosen via cross-validated feature selection, included five network
333 metrics across the three connectivity measures. For ICOH, the identified subset
334 selected was the betweenness centrality at ranges 11-13 and 19-21 Hz along-
335 side the clustering coefficient at a range of 15-17 Hz. The subset also included
336 the PSI average degree at 13-15 Hz and the WPLI variance degree from 1-3
337 Hz. These results indicate specifically which network metrics, from a machine-
338 learning perspective, contributed the most information for building an accurate
339 classification model. As such, the classifier was trained specifically, and only,
340 using these 5 key metrics. An illustrative example of these 5 selected network
341 metrics (e.g. features) are shown in Figure 4 as scatter plots. When training
342 the classifier, these network features are used to identify the underlying patterns
343 not readily observed, and are incorporated into guiding the machine learning
344 algorithm.

345 The resulting confusion matrix from the 5-fold cross-validated, cost-sensitive
346 classification analysis is seen in Table 5.

347 The overall classification accuracy was defined as the number of true label
348 classes correctly predicted by the classifier, e.g. the true positive diagonal of
349 Table 5. Presently, approximately 36 of the 51 children’s cognitive class (e.g.
350 normal, mild/moderate CI, severe CI) were correctly predicted, giving a total
351 accuracy of the classifier at 70.6%. Using Table 2, an overall ‘cost-penalty’ value
352 was calculated at 38 points, based on the children who were misclassified, i.e.

CST analysis of cognition standard score measures			
Network Type	Network Measurement	Frequency Range(s) (Hz)	Correlation ($\bar{\tau} \pm SD$)
ICOH	Clustering Coefficient	15-17 Hz	$-0.290 \pm 0.000^{\dagger*}$
ICOH	Average Degree	–	–
ICOH	Variance of Degree	13-15 Hz	-0.200 ± 0.000
ICOH	Variance of Degree	21-23 Hz	-0.203 ± 0.000
ICOH	Betweenness Centrality	11-13 Hz	$-0.273 \pm 0.000^{\dagger*}$
ICOH	Betweenness Centrality	15-17 Hz	-0.241 ± 0.000
ICOH	Betweenness Centrality	19-21 Hz	-0.203 ± 0.000
PSI	Clustering Coefficient	–	–
PSI	Average Degree	13-15 Hz	-0.210 ± 0.000
PSI	Variance of Degree	15-17 Hz	$-0.277 \pm 0.000^{\dagger*}$
PSI	Variance of Degree	21-23 Hz	-0.217 ± 0.000
PSI	Betweenness Centrality	5-7 Hz	$0.204 \pm 0.000^*$
PSI	Betweenness Centrality	15-17 Hz	-0.248 ± 0.000
WPLI	Clustering Coefficient	1-3 Hz	$-0.236 \pm 0.000^*$
WPLI	Clustering Coefficient	17-19 Hz	$0.287 \pm 0.000^{\dagger*}$
WPLI	Average Degree	–	–
WPLI	Variance of Degree	1-3 Hz	$-0.236 \pm 0.000^*$
WPLI	Betweenness Centrality	–	–

Table 4: Summary of Kendall’s τ correlation trends between various graph metrics and the cognition standard scores using the Cluster-Span Threshold (CST). For all values $|\tau|$ was between 0.201 and 0.290; mean = 0.237 ± 0.033 , and uncorrected $p < 0.05$. Significant values across contiguous narrow-band frequencies have been grouped together for ease of interpretation.

[†] Significant with Bonferroni correction at the level of frequencies.

* Significant after partial correlation correction to age of subjects, via modified τ with uncorrected $p < 0.05$.

Confusion Matrix from Classification Results

		CI-Predicted Class		
		Normal	Mild/Mod.	Severe
CI-True Class	Normal	26	<i>2</i>	<i>3</i>
	Mild/Mod.	2	3	<i>2</i>
	Severe	1	<i>5</i>	7

Table 5: Resulting confusion matrix from the 5-fold cross-validated, cost-sensitive classification scheme for all $n = 51$ children based on costs in Table 2. Rows represent true class labels, with columns as the predicted labels from the classification. Bold values along the diagonal show true positive classification results, where actual and predicted cognitive classes were accurately identified. Italicized values indicate children predicted to have CI, i.e. mild/moderate or severe class, by the classification scheme.

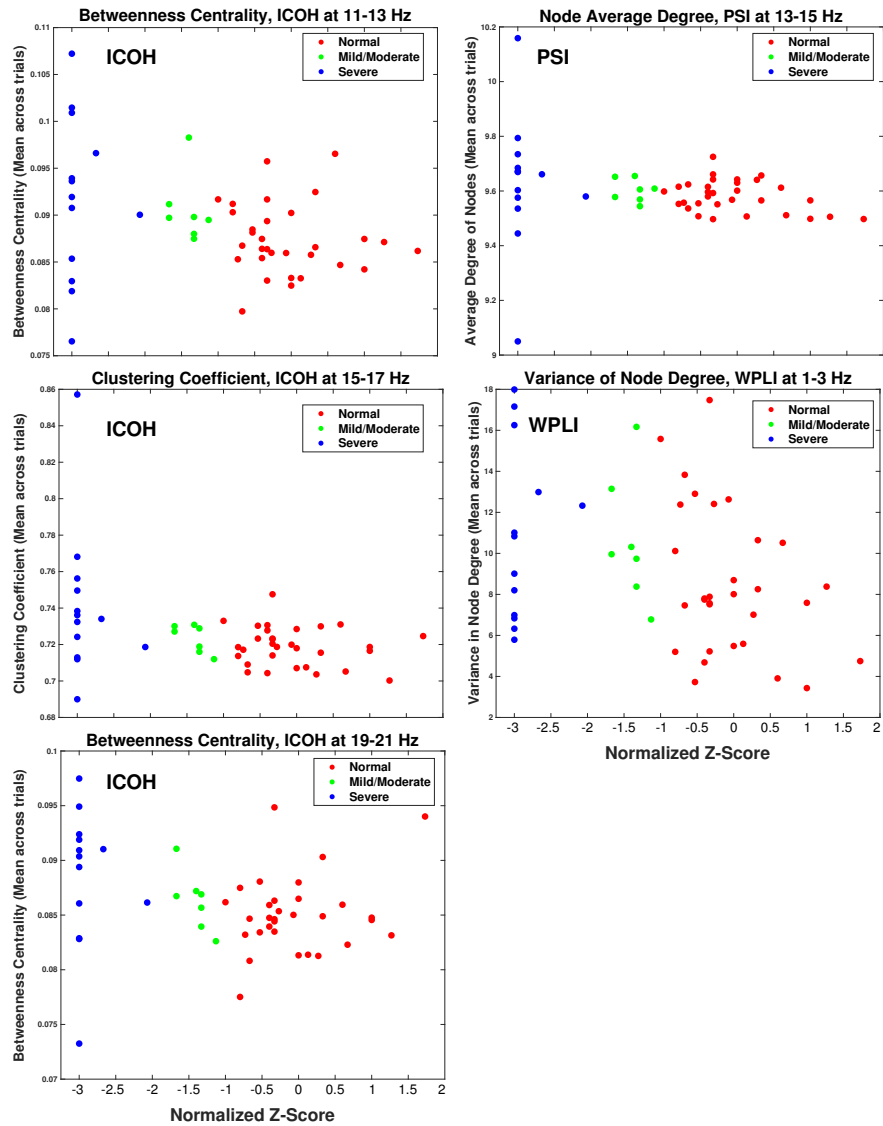


Figure 4: Scatter plot displaying the distribution of children for each of the 5 features used in training the KNN classification. Each panel displays network values on the y-axis, with the normalized cognition standard score (z-score) on the x-axis. Children classified into normal, mild/moderate CI and severe CI classes are displayed in red, green and blue respectively.

	Classification Scheme			
	Network Analysis	Random	Naive Class	Naive Value
Total Accuracy	70.6% (36/51)	45.4%(\approx 23/51)	Normal Cognition Mild/Moderate CI Severe CI	60.8% (31/51) 13.7% (7/51) 25.5% (13/51)
Total Cost Penalty	38 pts	\approx 65 pts	Normal Cognition Mild/Moderate CI Severe CI	100 pts 90.5 pts 84.5 pts

Table 6: Summary table of overall classification accuracies and total cost penalty for the proposed network analysis, random classification, and naive (single class) classification. Naive classification is split to show overall classification accuracy and cost penalties if all children were assigned as normal cognition, mild/moderate CI or severe CI classes. Total accuracy includes the approximate number of children with true positive predictions, out of total number of children evaluated.

353 their cognitive class was not correctly predicted.

354 The expected random classification accuracy is based on the distribution
355 of individuals belonging to each class, i.e. 31, 7 and 13 children for the *nor-*
356 *mal*, *mild/moderate* and *severe* classes respectively. Random accuracy would
357 be expected at 45.4%, with cost-penalty varying depending on misclassification
358 distributions. Using the average misclassification penalty and the percentage of
359 misidentified children (approximately 28 of the 51 subjects), the cost-penalty
360 would be at least 65 points.

361 The naive, or single-class, classification scheme assumed all subjects be-
362 longed to a single cognition class in order to calculate the accuracy and misclas-
363 sification costs under this scheme. For example, if all children were considered as
364 belonging to the ‘normal’ cognition class (i.e. naively classified as normal), then
365 exactly 31 of the 51 children (those whose true class is ‘normal’-the first row of
366 Table 5) would be correctly identified. This would give the naive classification
367 scheme an accuracy of 60.8%. Repeating this naive classification scheme for
368 mild/moderate and severe classes resulted in classification accuracies of 13.7%
369 (7/51), and 25.5% (13/51) respectively. Similarly, the total cost-penalty for
370 each naive classification would be 100, 90.5 and 84.5 points respectively, using
371 the same procedure and the penalty costs from Table 2.

372 Overall, the results indicate gains in classification accuracy and a reduced
373 total penalty as compared to both random and naive classification. This is
374 summarized in Table 6.

375 4. Discussion

376 The main finding of this study is demonstrating how graph analysis can be
377 exploited to identify potential computational biomarkers for CI in CWEOE di-
378 rectly from routinely collected clinical EEG. The results revealed a substantial
379 pool of potential network characteristics which might helpful in identifying CI in
380 CWEOE via several different network analysis and dependency combinations.
381 The breadth of these combinations emphasizes that network analysis of paediatric
382 EEG is well-suited for identifying possible CI markers in CWEOE. The

383 automated and quantitative nature of the processing chain, ability to appropri-
384 ately predict CI classes, and its use of routinely acquired EEG data make the
385 proposed methods an attractive proposition for clinical applications.

386 Flexibility in sensitivity and robustness of particular networks to features
387 of interest is an advantage of this analysis. For instance, the sensitivity of
388 phase-dependent connectivity measures, e.g. PSI and WPLI, was more preva-
389 lent compared to standard ICOH. This is not surprising as phase-oriented mea-
390 sures were developed to improve upon phase ambiguities in traditional ICOH
391 measurements [25, 28]. In addition, the sensitivity of PSI in picking up signifi-
392 cant correlations can be attributed in part to its equal treatment of small phase
393 differences in leading and lagging signals [25]. Such small phase differences con-
394 tribute equally in PSI, while counting for proportionally less in the WPLI by
395 definition [27, 26]. By construction, the WPLI results are substantially more
396 robust to noise and small perturbations in phase, through proportionally reflect-
397 ing phase differences in network connections with appropriate weights, providing
398 results for only large phase differences. Together these measures reflect trade-off
399 choices between sensitivity and robustness for network analysis.

400 Of interest for paediatric populations is the CST’s capability to identify
401 low frequency correlations in phase-dependent coherency measures. Both the
402 PSI and WPLI demonstrate sensitivity to lower frequencies, not present in the
403 ICOH or MST, in general. This is critical considering that in preschool chil-
404 dren lower frequencies typically contain the bands of interest present in adult
405 EEGs, e.g. the delta/theta/alpha bands [43, 44]. During development these
406 bands shift to higher frequencies [45], reflecting a large scale reorganization of
407 the endogenous brain electric fields and suggesting a transition to more func-
408 tionally integrated and coordinated neuronal activity [23]. The (low) chance of
409 all such significant findings being spurious is less detrimental than the potential
410 impact from disregarding these findings altogether. The ability to detect net-
411 work disruptions potentially present in these critical bands in CWEOE provides
412 high impact value, and the possibility for adjusting potential therapeutic and
413 treatment strategies for clinicians and researchers.

414 The identified subset of metrics for classification provide additional informa-
415 tion. All of the features in the subset reflected distribution measures of hub-like
416 network structures in the brain, relating to the balance between heterogene-
417 ity and centrality within the network. The implicated metrics, other than the
418 variance degree, corresponded to measures identifying local, centralized ‘criti-
419 cal’ nodes in a network. Their negative correlation to the cognition standard
420 scores imply that children with more locally centralized brain networks, and
421 consequently with less well distributed hub-like structures, are more likely to
422 have corresponding cognitive impairment. This is reasonable, since if there ex-
423 ists a small set of central, critical hubs responsible for communication across
424 the brain, disruption of these critical points (e.g. due to seizure activity and/or
425 diffuse damage in the brain) would have severely negative effects on commu-
426 nication connections. This is also supported by the negative correlation in the
427 variance degree metric in the WPLI. The variance degree can be interpreted as a
428 measure of a network’s heterogeneity [46]. As such, the negative variance degree

429 in the low (1-3 Hz) frequency range may reflect stunted cognitive development,
430 as normal maturation is associated with reduced activation in low frequencies
431 [47, 43, 48, 44, 49], implying a decrease in local connectivity and heterogeneity
432 of the networks. This compliments the above conclusions, suggesting a sensitiv-
433 ity in the likely well-centralized networks to significant disruptions by epilepsy.
434 The disrupted networks may then be reflected by the continued heterogeneity
435 and local connectivity of low frequency structures in impaired children.

436 Being able to predict the likely extent of CI using the identified markers
437 could provide an advantageous tool for clinicians. Specifically, being able to pair
438 specific network features to an effective prediction of CI would allow clinicians
439 to retain interpretation of the chosen network features while providing a tool to
440 quickly and objectively separate similar cases. To this end, the cost-sensitive,
441 simple KNN classifier explored in this work illustrates an early step towards this
442 aim.

443 Evaluating the network-based classifier results show the analysis was suc-
444 cessful at two levels. First, the proposed classifier was able to generally iden-
445 tify cognitively normal children from impaired children, when grouping the
446 mild/moderate CI and severe CI classes. This is seen in the first column of
447 Table 5 where only three impaired children are misidentified as ‘normal cogni-
448 tion’, giving a sensitivity of 85%. In other words, 17 of the 20 actual impaired
449 children were correctly identified as belonging to either the mild/moderate or
450 severe CI classes, demonstrating that the proposed network analysis and clas-
451 sifier was largely successful with respect to predicting children with some form
452 of impaired cognition, based on using the standard score definition. Similarly,
453 only five normal children were misidentified as generally impaired (i.e. classified
454 to either the mild/moderate or severe CI classes; top row of Table 5), giving a
455 specificity of approximately 84% (26/31) for appropriately identifying children
456 in the range of normal cognition. In addition, the network coupled classifier
457 was able to separate out cases of mild/moderate impairment from severe im-
458 pairment decently, with $> 50\%$ of impaired children correctly predicted. Thus,
459 the proposed classifier and associated methods provide considerable sensitivity
460 (85%) and specificity (84%) for clinicians in determining potential CI, while still
461 remaining relatively accurate in separating CI according to severity.

462 Statistical analysis in this manuscript was utilized as a first-pass means to
463 reduce the potential feature space for classification. Through identifying po-
464 tentially significant networks of interest, the number of features to test in the
465 classification step was substantially reduced. Through the statistical analysis,
466 pertinent features from a relevant and manageable feature space were selected.
467 It bears repeating that Kendall’s τ was a non-parametric significance test, which
468 means it did not rely on an underlying assumption of a normal (or any other)
469 distribution in the data. Kendall’s τ correlation was therefore robust to the
470 apparent flooring effect seen in the severe CI class, as it utilized concordant
471 and discordant pairs. As such, the conclusions drawn from the statistical anal-
472 ysis were unaffected by this phenomena. Future endeavours could refine such
473 features, based on different choices for the statistical analysis. Using a more
474 rigid/flexible analysis could lead to further culling/relaxation of the feature

475 space and provide an adjustable framework for examining network property
476 changes in CWEOE. Other future work could include alternative narrow-band
477 frequency binning and less strict automated rejection methods. Significant cor-
478 relations across sets of consecutive (and nearly consecutive) frequency bands
479 indicate likely targets for other potential follow-up studies.

480 The KNN classifier utilized in this study is a well-established classification
481 scheme [50], chosen *a priori* to help promote easier understanding of the classifi-
482 cation results in this pilot study. Its simplicity in implementation helps support
483 repeatability in the analysis methods for clinicians and researchers who may not
484 be as experienced in implementing more sophisticated classification paradigms.
485 Of course future developments to the described methods could include inte-
486 grating more complex classification schemes, such as deep convolutional neural
487 networks (dCNN) [51, 52, 53]. Utilizing dCNN in context with the presented
488 results, however, may require a significant amount of data to function well and
489 reduce the straight-forward interpretation of how the classification was calcu-
490 lated (although this may change in coming years- interested readers should see
491 [53]). Nevertheless, including such classification schemes could help improve the
492 results, especially at the second tier discrimination, e.g. at the level of discern-
493 ing between the cognitive impairment types (e.g. mild/moderate CI from severe
494 CI). A thorough investigation into incorporating and comparing additional clas-
495 sifiers thus is a strong potential avenue for expansion of this research.

496 The NEUROPROFILE cohort was advantageous in that formal neuropsy-
497 chological testing was coupled with EEG recordings, making it ideal for this
498 investigation. However, there are study limitations. Although this study used
499 routine clinical EEGs used in the diagnosis of incidence cases of CWEOE,
500 the three classes of normal, mild/moderate and severe impairment were un-
501 balanced; this occurred naturally. The majority of the sample was taken from
502 a population-based cohort, and mitigating potential influences from imbalanced
503 data was taken into account as much as possible when conducting the research,
504 e.g. through cost-sensitive analysis. Imbalanced data is not uncommon, but
505 the unbalanced distribution of CI in the current study reflects findings in a true
506 population-based cohort [20]. Furthermore, trialling this methodology in older
507 children with epilepsy may be an avenue for future studies, to provide further
508 insights as to the relationship between aetiology and CI, as well as provide
509 additional replications of the proposed techniques.

510 **5. Limitations**

511 Within the studied cohort of CWEOE, the epilepsy type and aetiologies were
512 heterogenous. Thus we are unable to determine if the model and methods used
513 have greater or lesser predictive value in specific subsets. Testing in a larger,
514 more homogeneous sample would provide clarification.

515 A gender disparity was noted within the normal cognition and mild/moderate
516 CI groups. Although this study reflects a true population, further studies are
517 needed to investigate this phenomena.

518 Note that the spectral components in the very low frequency narrow band
519 (e.g.1-3 Hz) may not be fully reliable due to the small epoch length, i.e. two
520 seconds. Information gained from the very low frequency band needs to be
521 interpreted with some care, as spurious connections are more likely to be present.
522 Again, however, the large number of trial epochs averaged for each child helped
523 mitigate these potential spurious connections.

524 We recognize a limitation in the assumption of dependency between the
525 frequency bins. While there is likely a strong local family dependency between
526 the narrow bins, the endpoints on the chosen frequency spectrum may not have
527 as strong of a relation. Therefore, significance at these level should be considered
528 carefully as they are more likely to be a false positive. However, the robust
529 nature of τ and chosen features from a machine-learning perspective help to
530 moderate potential impacts from this assumption on the presented results.

531 The use of a data-driven, narrow band approach in the analysis had a trade-
532 off of not using patient-specific frequency ranges for each child. Future studies
533 could be done to investigate how individualized frequencies, e.g. using individ-
534 ual alpha frequencies (IAF), could be aligned, interpreted and correlated when
535 assessing network abnormalities in the CWEOE population.

536 Only a small set of the available network analysis methods were explored in
537 this analysis. These were chosen prior to starting the project in order to limit
538 potential multiple comparisons and focus the study on a select few state-of-
539 the-art techniques. The selected dependency metrics (e.g. ICOH, PSI, WPLI)
540 and sub-network graphs (MST, CST) in this study are by no means a compre-
541 hensive set. Other network analysis techniques and measures of dependencies
542 offer potential avenues to further explore techniques which could help identify
543 CI in CWEOE. For other potential network analysis methods, the authors refer
544 interested readers to recent reviews [54, 55] covering the extensive available
545 techniques utilizing network analysis in brain signal processing.

546 **6. Conclusions**

547 This study explored processing EEG using network analysis to demonstrate
548 its use in identifying markers of CI in CWEOE for the first time. Results from
549 the study demonstrate these network markers in identifying critical structures of
550 CWEOE with CI and illustrate their potential predictive abilities using prelimi-
551 nary classification techniques. Replication of the identified methods using other
552 datasets, with alternative narrow-band frequency binning, less strict automated
553 rejection methods, and including correlations with brain MRI abnormalities may
554 bolster the generalizability and applicability of the proposed techniques.

555 **7. Acknowledgements**

556 The authors would like to thank the patients and families who participated
557 in the NEUROPROFILES [20] study. Funding support for this project was
558 provided by the RS McDonald Trust, Thomas Theodore Scott Ingram Memorial
559 Fund, and the Muir Maxwell Trust.

560 **8. Author Contributions**

561 Javier Escudero and Richard FM Chin conceived of the presented ideas. Eli
562 Kinney-Lang developed the theory, performed data analysis and interpretation,
563 and designed the computational framework of the project under supervision
564 of Richard FM Chin and Javier Escudero. Jay Shetty, Krishnaraya Kamath
565 Tallur, Michael Yoong and Ailsa McLellan were involved in the methodology
566 and collection of the original NEUROPROFILES dataset, including recruiting
567 patients and requesting and reporting patient EEGs. Matthew Hunter was the
568 lead author and investigator for the NEUROPROFILES project with senior
569 supervision under Richard FM Chin. Eli Kinney-Lang wrote the manuscript
570 and figures, with revision and comments provided by Matthew Hunter, Michael
571 Yoong, Jay Shetty, Krishnaraya Kamath Tallur, Ailsa McLellan, Richard FM
572 Chin and Javier Escudero. Final approval of this publication was provided by
573 all authors.

574 **Conflict of Interest Statement**

575 None of the authors have potential conflicts of interest to be disclosed.

576 **References**

- 577 [1] B. S. Chang, D. H. Lowenstein, *Epilepsy*, N. Engl. J. Med. 349 (2003)
578 1257–1266. doi:10.1056/NEJMra022308.
- 579 [2] C. Reilly, P. Atkinson, K. B. Das, R. F. M. C. Chin, S. E. Aylett, V. Burch,
580 C. Gillberg, R. C. Scott, B. G. R. Neville, Neurobehavioral comorbidities in
581 children with active epilepsy: a population-based study., *Pediatrics* 133 (6)
582 (2014) e1586–93. doi:10.1542/peds.2013–3787.
583 URL <http://www.ncbi.nlm.nih.gov/pubmed/24864167>
- 584 [3] C. Reilly, P. Atkinson, K. B. Das, R. F. Chin, S. E. Aylett, V. Burch,
585 C. Gillberg, R. C. Scott, B. G. Neville, Factors associated with quality of
586 life in active childhood epilepsy: A population-based study, *Eur. J. Paedi-*
587 *atr. Neurol.* 19 (3) (2015) 308–313. doi:10.1016/J.EJPN.2014.12.022.
588 URL <https://www.sciencedirect.com/science/article/pii/S1090379815000069>
- 590 [4] E.-H. Kim, T.-S. Ko, Cognitive impairment in childhood onset epilepsy:
591 up-to-date information about its causes., *Korean J. Pediatr.* 59 (4) (2016)
592 155–64. doi:10.3345/kjp.2016.59.4.155.
593 URL <http://www.ncbi.nlm.nih.gov/pubmed/27186225><http://www.pubmedcentral.nih.gov/articlerender.fcgi?artid=PMC4865638>
- 595 [5] K. Rantanen, K. Eriksson, P. Nieminen, Cognitive impairment in preschool
596 children with epilepsy, *Epilepsia* 52 (8) (2011) 1499–1505. doi:10.1111/
597 j.1528-1167.2011.03092.x.
598 URL <http://doi.wiley.com/10.1111/j.1528-1167.2011.03092.x>

- 599 [6] D. B. Bailey, Critical thinking about critical periods (2001).
- 600 [7] W. A. Hauser, J. F. Annegers, W. A. Rocca, Descriptive Epidemiology of
601 Epilepsy: Contributions of Population-Based Studies From Rochester, Min-
602 nesota, *Mayo Clin. Proc.* 71 (6) (1996) 576–586. doi:10.4065/71.6.576.
603 URL [https://www.sciencedirect.com/science/article/pii/](https://www.sciencedirect.com/science/article/pii/S0025619611641153)
604 [S0025619611641153](http://linkinghub.elsevier.com/retrieve/pii/S0025619611641153)[http://linkinghub.elsevier.com/retrieve/](http://linkinghub.elsevier.com/retrieve/pii/S0025619611641153)
605 [pii/S0025619611641153](http://linkinghub.elsevier.com/retrieve/pii/S0025619611641153)
- 606 [8] B. Neville, Epilepsy in childhood., *BMJ Br. Med. J.* 315 (1997) 924–930.
607 URL [https://www.ncbi.nlm.nih.gov/pmc/articles/PMC2127609/](https://www.ncbi.nlm.nih.gov/pmc/articles/PMC2127609/pdf/9361544.pdf)
608 [pdf/9361544.pdf](http://www.ncbi.nlm.nih.gov/pmc/articles/PMC2127609/pdf/9361544.pdf)[http://www.ncbi.nlm.nih.gov/pmc/articles/](http://www.ncbi.nlm.nih.gov/pmc/articles/PMC2127609/pdf/9361544.pdf)
609 [PMC2127609/](http://www.ncbi.nlm.nih.gov/pmc/articles/PMC2127609/pdf/9361544.pdf)
- 610 [9] M. J. England, C. T. Liverman, A. M. Schultz, L. M. Strawbridge, Epilepsy
611 across the spectrum: Promoting health and understanding. A summary of
612 the Institute of Medicine report (2012). doi:10.1016/j.yebeh.2012.06.
613 016.
- 614 [10] A. R. Brooks-Kayal, K. G. Bath, A. T. Berg, A. S. Galanopoulou, G. L.
615 Holmes, F. E. Jensen, A. M. Kanner, T. J. O’Brien, V. H. Whittemore,
616 M. R. Winawer, M. Patel, H. E. Scharfman, Issues related to symptomatic
617 and disease-modifying treatments affecting cognitive and neuropsychiatric
618 comorbidities of epilepsy, *Epilepsia* 54 (2013) 44–60. doi:10.1111/epi.
619 12298.
620 URL <http://doi.wiley.com/10.1111/epi.12298>
- 621 [11] M. Yoong, Quantifying the deficit-imaging neurobehavioural impairment
622 in childhood epilepsy., *Quant. Imaging Med. Surg.* 5 (2) (2015) 225–37.
623 doi:10.3978/j.issn.2223-4292.2015.01.06.
624 URL <http://www.ncbi.nlm.nih.gov/pubmed/25853081>[http://www.](http://www.ncbi.nlm.nih.gov/pubmed/25853081)
625 [pubmedcentral.nih.gov/articlerender.fcgi?artid=PMC4379313/](http://www.ncbi.nlm.nih.gov/pubmed/25853081)
626 [pmc/articles/PMC4379313/?report=abstract](http://www.ncbi.nlm.nih.gov/pubmed/25853081)
- 627 [12] C. J. Stam, J. C. Reijneveld, Graph theoretical analysis of complex net-
628 works in the brain, *Nonlinear Biomed. Phys.* 1 (1) (2007) 3. doi:10.1186/
629 1753-4631-1-3.
630 URL [http://nonlinearbiomedphys.biomedcentral.com/articles/10.](http://nonlinearbiomedphys.biomedcentral.com/articles/10.1186/1753-4631-1-3)
631 [1186/1753-4631-1-3](http://nonlinearbiomedphys.biomedcentral.com/articles/10.1186/1753-4631-1-3)
- 632 [13] E. Bullmore, O. Sporns, Complex brain networks: graph theoretical analy-
633 sis of structural and functional systems, *Nat. Rev. Neurosci.* 10 (4) (2009)
634 312–312. arXiv:arXiv:1011.1669v3, doi:10.1038/nrn2618.
635 URL <http://www.nature.com/doifinder/10.1038/nrn2618>
- 636 [14] E. van Diessen, W. M. Otte, C. J. Stam, K. P. Braun, F. E. Jansen,
637 Electroencephalography based functional networks in newly diagnosed
638 childhood epilepsies, *Clin. Neurophysiol.* 127 (6) (2016) 2325–2332.
639 doi:10.1016/j.clinph.2016.03.015.

- 640 URL [http://linkinghub.elsevier.com/retrieve/pii/
641 S1388245716001085](http://linkinghub.elsevier.com/retrieve/pii/S1388245716001085)
- 642 [15] F. Vecchio, F. Miraglia, F. Piludu, G. Granata, R. Romanello, M. Caulo,
643 V. Onofrj, P. Bramanti, C. Colosimo, P. M. Rossini, Small World architec-
644 ture in brain connectivity and hippocampal volume in Alzheimer’s disease:
645 a study via graph theory from EEG data, *Brain Imaging Behav.* 11 (2)
646 (2017) 473–485. doi:10.1007/s11682-016-9528-3.
647 URL <http://link.springer.com/10.1007/s11682-016-9528-3>
- 648 [16] F. Vecchio, F. Miraglia, P. Maria Rossini, Connectome: Graph theory
649 application in functional brain network architecture, *Clin. Neurophysiol.*
650 *Pract.* 2 (2017) 206–213. doi:10.1016/J.CNP.2017.09.003.
651 URL [https://www.sciencedirect.com/science/article/pii/
652 S2467981X17300276](https://www.sciencedirect.com/science/article/pii/S2467981X17300276)
- 653 [17] B. Tóth, G. Urbán, G. P. Hádén, M. Márk, M. Török, C. J. Stam,
654 I. Winkler, Large-scale network organization of EEG functional connec-
655 tivity in newborn infants, *Hum. Brain Mapp.* 38 (8) (2017) 4019–4033.
656 doi:10.1002/hbm.23645.
657 URL <http://doi.wiley.com/10.1002/hbm.23645>
- 658 [18] C. J. Stam, Modern network science of neurological disorders, *Nat. Rev.*
659 *Neurosci.* 15 (10) (2014) 683–695. arXiv:arXiv:1011.1669v3, doi:10.
660 1038/nrn3801.
661 URL <http://www.nature.com/doifinder/10.1038/nrn3801>
- 662 [19] M. Yoong, M. Hunter, J. Stephen, A. Quigley, J. Jones, J. Shetty,
663 A. Mclellan, M. E. Bastin, R. F. M. Chin, Cognitive impairment in early
664 onset epilepsy is associated with reduced left thalamic volume, *Epilepsy*
665 *Behav.* doi:10.1016/j.yebeh.2018.01.018.
666 URL [https://www.epilepsybehavior.com/article/S1525-5050\(17\)
667 30945-9/pdf](https://www.epilepsybehavior.com/article/S1525-5050(17)30945-9/pdf)
- 668 [20] H. M.B., S. R., V. K., Y. M., M. A., S. J., C. R.F., NEUROde-
669 velopment in PReschool Children Of Fife and Lothian Epilepsy
670 Study: NEUROPROFILES - A population-based study (2015).
671 doi:http://dx.doi.org/10.1111/epi.12675.
672 URL [http://ovidsp.ovid.com/ovidweb.cgi?T=JS{&}PAGE=
673 reference{&}D=emed12{&}NEWS=N{&}AN=71754114](http://ovidsp.ovid.com/ovidweb.cgi?T=JS{&}PAGE=reference{&}D=emed12{&}NEWS=N{&}AN=71754114)
- 674 [21] M. Friedman, The Use of Ranks to Avoid the Assumption of Normality
675 Implicit in the Analysis of Variance, *J. Am. Stat. Assoc.* 32 (200) (1937)
676 675. doi:10.2307/2279372.
677 URL <https://www.jstor.org/stable/2279372?origin=crossref>
- 678 [22] R. Oostenveld, P. Fries, E. Maris, J.-M. Schoffelen, FieldTrip: Open Source
679 Software for Advanced Analysis of MEG, EEG, and Invasive Electrophys-
680 iological Data, *Comput. Intell. Neurosci.* 2011 (2011) 1–9. arXiv:156869,

- 681 doi:10.1155/2011/156869.
682 URL <http://www.hindawi.com/journals/cin/2011/156869/>
- 683 [23] V. Miskovic, X. Ma, C.-A. Chou, M. Fan, M. Owens, H. Sayama, B. E.
684 Gibb, Developmental changes in spontaneous electrocortical activity and
685 network organization from early to late childhood., *Neuroimage* 118 (2015)
686 237–47. doi:10.1016/j.neuroimage.2015.06.013.
687 URL [http://linkinghub.elsevier.com/retrieve/pii/](http://linkinghub.elsevier.com/retrieve/pii/S1053811915005108)
688 [http://dx.doi.org/10.1016/j.neuroimage.](http://dx.doi.org/10.1016/j.neuroimage.2015.06.013)
689 [http://www.sciencedirect.com/science/article/](http://www.sciencedirect.com/science/article/pii/S1053811915005108)
690 [http://www.ncbi.nlm.nih.gov/pubmed/](http://www.ncbi.nlm.nih.gov/pubmed/26057595)
691 [26057595http://www.pubmedcentral.nih.gov](http://www.pubmedcentral.nih.gov)
- 692 [24] G. Nolte, O. Bai, L. Wheaton, Z. Mari, S. Vorbach, M. Hallett, Identifying true brain interaction from EEG data using the imaginary part of coherency, *Clin. Neurophysiol.* 115 (10) (2004) 2292–2307. doi:10.1016/j.clinph.2004.04.029.
- 696 [25] G. Nolte, A. Ziehe, V. V. Nikulin, A. Schlögl, N. Krämer, T. Brismar, K.-R. Müller, Robustly Estimating the Flow Direction of Information in Complex Physical Systems, *Phys. Rev. Lett.* 100 (23) (2008) 234101. arXiv:0712.2352, doi:10.1103/PhysRevLett.100.234101.
699 URL <https://link.aps.org/doi/10.1103/PhysRevLett.100.234101>
- 701 [26] C. J. Stam, G. Nolte, A. Daffertshofer, Phase lag index: Assessment of functional connectivity from multi channel EEG and MEG with diminished bias from common sources, *Hum. Brain Mapp.* 28 (11) (2007) 1178–1193. doi:10.1002/hbm.20346.
- 705 [27] M. Vinck, R. Oostenveld, M. Van Wingerden, F. Battaglia, C. M. A. Pennartz, An improved index of phase-synchronization for electrophysiological data in the presence of volume-conduction, noise and sample-size bias, *Neuroimage* 55 (4) (2011) 1548–1565. arXiv:0006269v1, doi:10.1016/j.neuroimage.2011.01.055.
709 URL <http://dx.doi.org/10.1016/j.neuroimage.2011.01.055>
- 711 [28] S. Haufe, V. V. Nikulin, K.-R. Müller, G. Nolte, A critical assessment of connectivity measures for EEG data: A simulation study, *Neuroimage* 64 (1) (2013) 120–133. doi:10.1016/j.neuroimage.2012.09.036.
714 URL <http://dx.doi.org/10.1016/j.neuroimage.2012.09.036><http://linkinghub.elsevier.com/retrieve/pii/S1053811912009469>
- 716 [29] P. Tewarie, E. van Dellen, A. Hillebrand, C. J. Stam, The minimum spanning tree: An unbiased method for brain network analysis, *Neuroimage* 104 (2015) 177–188. doi:10.1016/j.neuroimage.2014.10.015.
719 URL <http://dx.doi.org/10.1016/j.neuroimage.2014.10.015>
- 720 [30] A. Fornito, A. Zalesky, E. T. Bullmore, Network scaling effects in graph analytic studies of human resting-state fMRI data, *Front. Syst. Neurosci.*
- 721

- 722 4 (2010) 22. doi:10.3389/fnsys.2010.00022.
723 URL [http://journal.frontiersin.org/article/10.3389/fnsys.](http://journal.frontiersin.org/article/10.3389/fnsys.2010.00022/abstract)
724 2010.00022/abstract
- 725 [31] B. C. M. Van Wijk, C. J. Stam, A. Daffertshofer, Comparing Brain
726 Networks of Different Size and Connectivity Density Using Graph The-
727 orydoi:10.1371/journal.pone.0013701.
728 URL <http://www.nwo.nl>
- 729 [32] K. Smith, H. Azami, M. A. Parra, J. M. Starr, J. Escudero, Cluster-span
730 threshold: An unbiased threshold for binarising weighted complete net-
731 works in functional connectivity analysis, Proc. Annu. Int. Conf. IEEE Eng.
732 Med. Biol. Soc. EMBS 2015-Novem (2015) 2840–2843. arXiv:1604.02403,
733 doi:10.1109/EMBC.2015.7318983.
- 734 [33] J. B. Kruskal, On the Shortest Spanning Subtree of a Graph and the
735 Traveling Salesman Problem, Proc. Am. Math. Soc. 7 (1) (1956) 48.
736 arXiv:arXiv:1011.1669v3, doi:10.2307/2033241.
737 URL [https://www.ams.org/journals/proc/1956-007-01/](https://www.ams.org/journals/proc/1956-007-01/S0002-9939-1956-0078686-7/S0002-9939-1956-0078686-7.pdf)
738 S0002-9939-1956-0078686-7/S0002-9939-1956-0078686-7.pdf[http://](http://www.jstor.org/stable/2033241?origin=crossref)
739 www.jstor.org/stable/2033241?origin=crossref
- 740 [34] K. Smith, D. Abasolo, J. Escudero, Accounting for the complex hierarchical
741 topology of EEG phase-based functional connectivity in network binarisa-
742 tion, PLoS One.
- 743 [35] A. R. Gilpin, Table for Conversion of Kendall's Tau to Spearman's
744 Rho Within the Context of Measures of Magnitude of Effect for Meta-
745 Analysis, Educ. Psychol. Meas. 53 (1) (1993) 87–92. arXiv:0803973233,
746 doi:10.1177/0013164493053001007.
747 URL [http://epm.sagepub.com/cgi/doi/10.1177/](http://epm.sagepub.com/cgi/doi/10.1177/0013164493053001007)
748 [0013164493053001007](http://journals.sagepub.com/doi/10.1177/0013164493053001007)[http://journals.sagepub.com/doi/10.1177/](http://journals.sagepub.com/doi/10.1177/0013164493053001007)
749 [0013164493053001007](http://journals.sagepub.com/doi/10.1177/0013164493053001007)
- 750 [36] N. Shong, Pearson's versus Spearman's and Kendall's correlation coef-
751 ficients for continuous data, Ph.D. thesis (2010). arXiv:arXiv:1011.
752 1669v3, doi:10.1017/CB09781107415324.004.
- 753 [37] G. Fraga González, M. Van der Molen, G. Žarić, M. Bonte, J. Tijms,
754 L. Blomert, C. Stam, M. Van der Molen, Graph analysis of EEG resting
755 state functional networks in dyslexic readers, Clin. Neurophysiol. 127 (9)
756 (2016) 3165–3175. doi:10.1016/j.clinph.2016.06.023.
757 URL [http://linkinghub.elsevier.com/retrieve/pii/](http://linkinghub.elsevier.com/retrieve/pii/S1388245716304539)
758 [S1388245716304539](http://linkinghub.elsevier.com/retrieve/pii/S1388245716304539)
- 759 [38] M. Hall, E. Frank, G. Holmes, B. Pfahringer, P. Reutemann, I. H. Witten,
760 The WEKA data mining software, ACM SIGKDD Explor. 11 (1) (2009)
761 10–18. doi:10.1145/1656274.1656278.
762 URL <http://portal.acm.org/citation.cfm?doid=1656274.1656278>

763 delimiter"026E30F\$npapers2://publication/doi/10.1145/1656274.
764 1656278

765 [39] E. Frank, M. A. Hall, I. H. Witten, The WEKA Workbench, in: Morgan
766 Kaufmann, Fourth Ed., Elsevier, 2016, pp. 553–571.
767 URL [http://www.cs.waikato.ac.nz/ml/weka/
768 Witten{}_et{}_al{}_2016{}_appendix.pdf](http://www.cs.waikato.ac.nz/ml/weka/Witten{}_et{}_al{}_2016{}_appendix.pdf)

769 [40] S. Khalid, T. Khalil, S. Nasreen, A survey of feature selection and feature
770 extraction techniques in machine learning, in: 2014 Sci. Inf. Conf., IEEE,
771 2014, pp. 372–378. doi:10.1109/SAI.2014.6918213.
772 URL [http://ieeexplore.ieee.org/lpdocs/epic03/wrapper.htm?
773 arnumber=6918213](http://ieeexplore.ieee.org/lpdocs/epic03/wrapper.htm?arnumber=6918213)

774 [41] Z.-H. Zhou, X.-Y. Liu, On multi-class cost-sensitive learning, *Comput.*
775 *Intell.* 26 (3) (2010) 232–257. doi:10.1111/j.1467-8640.2010.00358.x.
776 URL [https://www.scopus.com/inward/record.uri?eid=2-s2.
777 0-77955034751&doi=10.1111/j.1467-8640.2010.00358.
778 x&partnerID=40&md5=21d7f85735dd6b67beeb0f73e6177cf7](https://www.scopus.com/inward/record.uri?eid=2-s2.0-77955034751&doi=10.1111/j.1467-8640.2010.00358.x&partnerID=40&md5=21d7f85735dd6b67beeb0f73e6177cf7)

779 [42] J. Shao, Bootstrap Model Selection, *J. Am. Stat. Assoc.* 91 (434) (1996)
780 655–665. doi:10.2307/2291661.
781 URL [http://www.jstor.org/stable/2291661\\$
782 delimiter"026E30F\\$nhhttps://www.jstor.org/stable/pdfplus/10.
783 2307/2291661.pdf?acceptTC=true](http://www.jstor.org/stable/2291661)

784 [43] P. J. Marshall, Y. Bar-Haim, N. A. Fox, Development of the EEG from 5
785 months to 4 years of age, *Clin. Neurophysiol.* 113 (8) (2002) 1199–1208.
786 doi:10.1016/S1388-2457(02)00163-3.
787 URL [http://www.sciencedirect.com/science/article/pii/
788 S1388245702001633](http://www.sciencedirect.com/science/article/pii/S1388245702001633)

789 [44] E. OREKHOVA, T. STROGANOVA, I. POSIKERA, M. ELAM, EEG
790 theta rhythm in infants and preschool children, *Clin. Neurophysiol.* 117 (5)
791 (2006) 1047–1062. doi:10.1016/j.clinph.2005.12.027.
792 URL [http://linkinghub.elsevier.com/retrieve/pii/
793 S1388245706000095](http://linkinghub.elsevier.com/retrieve/pii/S1388245706000095)

794 [45] A. Chiang, C. Rennie, P. Robinson, S. van Albada, C. Kerr, Age trends and
795 sex differences of alpha rhythms including split alpha peaks, *Clin. Neuro-*
796 *physiol.* 122 (8) (2011) 1505–1517. doi:10.1016/j.clinph.2011.01.040.
797 URL [http://linkinghub.elsevier.com/retrieve/pii/
798 S1388245711000903](http://linkinghub.elsevier.com/retrieve/pii/S1388245711000903)

799 [46] T. a. B. Snijders, The degree variance: An index of graph heterogeneity,
800 *Soc. Networks* 3 (3) (1981) 163–174. doi:10.1016/0378-8733(81)
801 90014-9.
802 URL [http://linkinghub.elsevier.com/retrieve/pii/
803 0378873381900149](http://linkinghub.elsevier.com/retrieve/pii/0378873381900149)

- 804 [47] M. Matsuura, K. Yamamoto, H. Fukuzawa, Y. Okubo, H. Uesugi, M. Mori-
805 iwa, T. Kojima, Y. Shimazono, Age development and sex differences of
806 various EEG elements in healthy children and adults—quantification by a
807 computerized wave form recognition method, *Electroencephalogr Clin Neu-*
808 *rophysiol* 60 (5) (1985) 394–406. doi:10.1016/0013-4694(85)91013-2.
809 URL <http://www.ncbi.nlm.nih.gov/pubmed/2580690>
- 810 [48] A. Amador, P. Valdés Sosa, R. Pascual Marqui, L. Garcia, R. Lirio, J. Ba-
811 yard, On the structure of EEG development, *Electroencephalogr. Clin.*
812 *Neurophysiol.* 73 (1) (1989) 10–19. doi:10.1016/0013-4694(89)90015-1.
813 URL [http://linkinghub.elsevier.com/retrieve/pii/](http://linkinghub.elsevier.com/retrieve/pii/0013469489900151)
814 [0013469489900151](http://linkinghub.elsevier.com/retrieve/pii/0013469489900151)
- 815 [49] T. Gasser, R. Verleger, P. Bächer, L. Sroka, Development of the
816 EEG of school-age children and adolescents. I. Analysis of band
817 power, *Electroencephalogr. Clin. Neurophysiol.* 69 (2) (1988) 91–99.
818 doi:10.1016/0013-4694(88)90204-0.
819 URL [http://linkinghub.elsevier.com/retrieve/pii/](http://linkinghub.elsevier.com/retrieve/pii/0013469488902040)
820 [0013469488902040](http://linkinghub.elsevier.com/retrieve/pii/0013469488902040)
- 821 [50] F. Lotte, L. Bougrain, A. Cichocki, M. Clerc, M. Congedo, A. Rako-
822 tomamonjy, F. Yger, A review of classification algorithms for EEG-
823 based brain-computer interfaces: A 10 year update (jun 2018).
824 doi:10.1088/1741-2552/aab2f2.
825 URL [http://stacks.iop.org/1741-2552/15/i=3/a=031005?key=](http://stacks.iop.org/1741-2552/15/i=3/a=031005?key=crossref.9cd2b15ab65c8ad34b475584b43dc509)
826 [crossref.9cd2b15ab65c8ad34b475584b43dc509](http://stacks.iop.org/1741-2552/15/i=3/a=031005?key=crossref.9cd2b15ab65c8ad34b475584b43dc509)
- 827 [51] R. Acharya, U. Rajendra Acharya, S. L. Oh, Y. Hagiwara, J. H. Tan,
828 H. Adeli, Deep convolutional neural network for the automated detection
829 and diagnosis of seizure using EEG signals PhD work View project
830 Segmentation of features in fundus image View project Deep convolutional
831 neural network for the automated detection and diagnosi, *Comput. Biol.*
832 *Med.* 100 (2017) 270–278. doi:10.1016/j.compbimed.2017.09.017.
833 URL [https://www.sciencedirect.com/science/article/pii/](https://www.sciencedirect.com/science/article/pii/S0010482517303153)
834 [S0010482517303153](https://www.sciencedirect.com/science/article/pii/S0010482517303153)[https://www.researchgate.net/publication/](https://www.researchgate.net/publication/320072603)
835 [320072603](https://www.researchgate.net/publication/320072603)
- 836 [52] M. Längkvist, L. Karlsson, A. Loutfi, A review of unsupervised
837 feature learning and deep learning for time-series modeling, *Pat-*
838 *tern Recognit. Lett.* 42 (1) (2014) 11–24. arXiv:1602.07261,
839 doi:10.1016/j.patrec.2014.01.008.
840 URL [https://www.sciencedirect.com/science/article/pii/](https://www.sciencedirect.com/science/article/pii/S0167865514000221)
841 [S0167865514000221](https://www.sciencedirect.com/science/article/pii/S0167865514000221)
- 842 [53] G. Montavon, W. Samek, K. R. Müller, Methods for interpreting and
843 understanding deep neural networks, *Digit. Signal Process. A Rev. J.* 73
844 (2018) 1–15. arXiv:1706.07979, doi:10.1016/j.dsp.2017.10.011.

- 845 URL [https://www.sciencedirect.com/science/article/pii/](https://www.sciencedirect.com/science/article/pii/S1051200417302385)
846 [S1051200417302385](https://www.sciencedirect.com/science/article/pii/S1051200417302385)
- 847 [54] G. C. O'Neill, P. Tewarie, D. Vidaurre, L. Liuzzi, M. W. Wool-
848 rich, M. J. Brookes, Dynamics of large-scale electrophysiological
849 networks: A technical review, *Neuroimage* 180 (2018) 559–576.
850 doi:10.1016/j.neuroimage.2017.10.003.
851 URL [https://www.sciencedirect.com/science/article/pii/](https://www.sciencedirect.com/science/article/pii/S1053811917308169)
852 [S1053811917308169](https://www.sciencedirect.com/science/article/pii/S1053811917308169)
- 853 [55] F. Rosenow, N. van Alphen, A. Becker, A. Chiocchetti, R. Deichmann,
854 T. Deller, T. Freiman, C. M. Freitag, J. Gehrig, A. M. Hermsen, P. Jedlicka,
855 C. Kell, K. M. Klein, S. Knake, D. M. Kullmann, S. Liebner, B. A. Nor-
856 wood, D. Omigie, K. Plate, A. Reif, P. S. Reif, Y. Reiss, J. Roeper,
857 M. W. Ronellenfisch, S. Schorge, G. Schratt, S. W. Schwarzacher, J. P.
858 Steinbach, A. Strzelczyk, J. Triesch, M. Wagner, M. C. Walker, F. von
859 Wegner, S. Bauer, Personalized translational epilepsy research: Novel
860 approaches and future perspectives, *Epilepsy Behav.* 76 (2017) 13–18.
861 doi:10.1016/j.yebeh.2017.06.041.
862 URL [https://www.sciencedirect.com/science/article/pii/](https://www.sciencedirect.com/science/article/pii/S1525505017304596)
863 [S1525505017304596](https://www.sciencedirect.com/science/article/pii/S1525505017304596)
- 864 [56] C. J. Stam, Nonlinear dynamical analysis of EEG and MEG: Review of an
865 emerging field (oct 2005). doi:10.1016/j.clinph.2005.06.011.
866 URL [http://linkinghub.elsevier.com/retrieve/pii/](http://linkinghub.elsevier.com/retrieve/pii/S1388245705002403)
867 [S1388245705002403](http://linkinghub.elsevier.com/retrieve/pii/S1388245705002403)
- 868 [57] J. Cabral, M. L. Kringelbach, G. Deco, Exploring the network dynamics
869 underlying brain activity during rest, *Prog. Neurobiol.* 114 (2014) 102–131.
870 doi:10.1016/j.pneurobio.2013.12.005.
871 URL <http://dx.doi.org/10.1016/j.pneurobio.2013.12.005>
- 872 [58] M.-T. Horstmann, S. Bialonski, N. Noennig, H. Mai, J. Prusseit,
873 J. Wellmer, H. Hinrichs, K. Lehnertz, State dependent properties of epilep-
874 tic brain networks: comparative graph-theoretical analyses of simultane-
875 ously recorded EEG and MEG., *Clin. Neurophysiol.* 121 (2) (2010) 172–85.
876 doi:10.1016/j.clinph.2009.10.013.
877 URL <http://www.ncbi.nlm.nih.gov/pubmed/20045375>
- 878 [59] P. L. Nunez, R. Srinivasan, A. F. Westdorp, R. S. Wijesinghe, D. M.
879 Tucker, R. B. Silberstein, P. J. Cadusch, EEG coherency I: Statistics,
880 reference electrode, volume conduction, Laplacians, cortical imag-
881 ing, and interpretation at multiple scales 103 (5) (1997) 499–515.
882 doi:10.1016/S0013-4694(97)00066-7.
883 URL [http://linkinghub.elsevier.com/retrieve/pii/](http://linkinghub.elsevier.com/retrieve/pii/S0013469497000667)
884 [S0013469497000667](http://linkinghub.elsevier.com/retrieve/pii/S0013469497000667)

885 **Appendix A. Network Coupling Definitions**

886 Appendix A outlines the key network definitions and details for the presented
 887 analysis. For in-depth reviews see [56, 13], and for further reading [12, 57, 58].

888 *Cross-spectrum*

Functional EEG connections are established through measures of interde-
 pendency between signals s_i and s_j [58] for any pair of EEG channels i and
 j . A common measurement for examining this interdependency is the cross-
 spectrum function $S_{ij}(f)$ [59, 24, 58]. Formally, let $x_i(f)$ and $x_j(f)$ be the
 complex Fourier transforms of the time series signals s_i and s_j for any pair (i, j)
 of EEG channels. Then the cross-spectrum can be calculated as

$$S_{ij}(f) \equiv \langle x_i(f)x_j^\dagger(f) \rangle \quad (\text{A.1})$$

889 where \dagger indicates the complex conjugation, and $\langle \rangle$ refers to the expectation value
 890 (also written as $E\{\}$) [24].

891 *Imaginary Part of Coherency (ICOH)*

Coherency is defined as the normalized cross-spectrum[24]:

$$C_{ij}(f) \equiv \frac{S_{ij}(f)}{(S_{ii}(f)S_{jj}(f))^{1/2}} \quad (\text{A.2})$$

Therefore, the imaginary part of coherency is defined as [24]

$$ICoh_{ij}(f) \equiv Im\{C_{ij}(f)\} \quad (\text{A.3})$$

892 where $Im\{\}$ refers to taking the imaginary part of a value, in this case the
 893 complex coherency measure.

894 *Phase-Slope Index (PSI)*

The PSI is defined as:

$$\Psi_{ij}(f) = Im\left\{\sum_{f \in F} C_{ij}^\dagger(f)C_{ij}(f + \delta f)\right\} \quad (\text{A.4})$$

895 where $C_{ij}(f)$ is as defined in equation A.2, δf is the frequency resolution, and
 896 $f \in F$ is the set of frequencies over which the phase-slope is calculated. See [25]
 897 for details.

898 *Phase-Lag Index*

The PLI is defined as: [26, 27]

$$\Theta_{ij} \equiv |\langle sign(Im\{S_{ij}(f)\}) \rangle| \quad (\text{A.5})$$

899 where $sign(\cdot)$ is the positive or negative sign, and $Im\{S_{ij}(f)\}$ is the imaginary
900 part of the cross-spectrum. Note that ICOH in equation (A.3) reflects the imag-
901 inary part of the *normalized* cross-spectrum, while the standard cross-spectrum
902 is used here.

903 *Weighted Phase-Lag Index (WPLI)*

The weighted PLI (WPLI) is defined as: [27]

$$\Phi_{ij}(f) \equiv \frac{|\langle |S| sign(S) \rangle|}{\langle |S| \rangle} \quad (\text{A.6})$$

904 where $S = Im\{S_{ij}(f)\}$.

905 **Appendix B. Supplementary Figures**

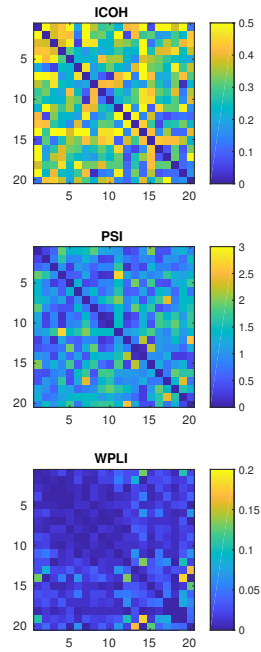


Figure B.5: Adjacency matrices for a representative 'normal cognition' child calculated by ICOH, PSI and WPLI between the 5-9 Hz frequency range.

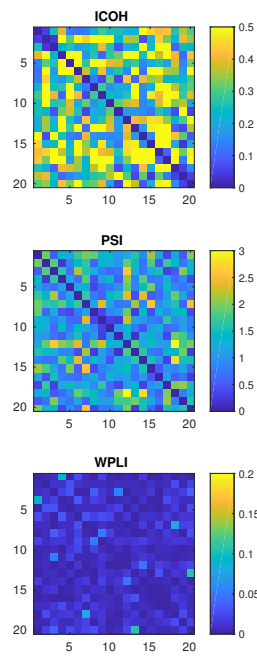


Figure B.6: Adjacency matrices for a representative 'impaired cognition' child calculated by ICOH, PSI and WPLI between the 5-9 Hz frequency range.